

# Iron oxide nanocomposite magnets produced by partial reduction of strontium hexaferrite

Jussi Tikkanen<sup>1,2,a</sup> and Petriina Paturi<sup>1</sup>

<sup>1</sup>Wihuri Physical Laboratory, Department of Physics and Astronomy, University of Turku, FI-20014, Finland

<sup>2</sup>University of Turku Graduate School (UTUGS), University of Turku, FI-20014, Finland

**Abstract.** Isotropic bulk nanocomposite permanent magnets were produced with strontium hexaferrite, SrO·6Fe<sub>2</sub>O<sub>3</sub>, and magnetite, Fe<sub>3</sub>O<sub>4</sub>, as the magnetically hard and soft components. A novel synthesis scheme based on the partial reduction of SrO·6Fe<sub>2</sub>O<sub>3</sub> was employed. In two parallel experiments, nano- and microcrystalline SrO·6Fe<sub>2</sub>O<sub>3</sub> particles were compacted into pellets along with a controlled, understoichiometric amount of potato starch as a reducing agent. The pellets were then sintered in a passive atmosphere. Based on XRD and room temperature magnetic hysteresis measurements, it was concluded that a fraction of the SrO·6Fe<sub>2</sub>O<sub>3</sub> input material had been reduced into Fe<sub>3</sub>O<sub>4</sub>. In comparison with pure SrO·6Fe<sub>2</sub>O<sub>3</sub> control pellets, these composites exhibited maximum energy product increases in excess of 5 % due to remanence boosting. The improvement of magnetic properties was attributed to an efficient exchange spring coupling between the magnetic phases. Interestingly, as the synthesis scheme also worked for microcrystalline SrO·6Fe<sub>2</sub>O<sub>3</sub>, the method could presumably be adapted to yield crystallographically oriented bulk nanocomposite magnets.

## 1 Introduction

Despite the impressive performance characteristics of rare-earth permanent magnets, the considerably cheaper magnetoplumbite (M) ferrites barium hexaferrite, BaO·6Fe<sub>2</sub>O<sub>3</sub>, and strontium hexaferrite, SrO·6Fe<sub>2</sub>O<sub>3</sub>, remain the hard magnetic materials of choice for a majority of everyday applications. A great deal of research has been targeted on the improvement of these magnetic derivatives of iron(III) oxide, and although some progress has been made in terms of maximum energy products,  $BH_{\max}$ , by introducing suitable dopant chemicals like La and Co, it seems that the conventional evolution of ferrite magnets is approaching its practical boundaries [1].

One novel way to improve upon the properties of M-ferrites would be to combine them heterogeneously with other magnetic materials with useful complementary properties, to produce composite permanent magnets. In this paper, work regarding the rather natural combination of strontium hexaferrite, SrO·6Fe<sub>2</sub>O<sub>3</sub>, and magnetite, Fe<sub>3</sub>O<sub>4</sub>, a magnetically softer ferrite, is reported. Whereas SrO·6Fe<sub>2</sub>O<sub>3</sub> is renowned for its high magnetic anisotropy ( $K_1 = 350 \text{ kJ m}^{-3}$  [2]) but is somewhat short on saturation magnetization ( $M_s = 380 \text{ kA m}^{-1}$  [2]), Fe<sub>3</sub>O<sub>4</sub> would bring in more magnetization ( $M_s = 480 \text{ kA m}^{-1}$  [2]) provided that some external mechanism could be utilized to boost its nearly nonexistent coercivity sufficiently to retain a high remanence, a centrally important property for any permanent magnet [2].

One such coercivity mechanism, the *exchange spring*, was theoretically described by Kneller and Hawig in 1991 [3]. To summarize, the mechanism requires a nanocomposite of the magnetically hard and soft phases to be constructed in such a manner that a maximal volume fraction of the soft component lies within the exchange length [2]

$$l_{\text{ex}} = \sqrt{\frac{A}{\mu_0 M_s^2}} \quad (1)$$

of the hard component. Here  $A$  is the exchange stiffness of the hard phase, roughly proportional to its Curie temperature.  $\mu_0$  and  $M_s$  represent vacuum permeability and saturation magnetization, respectively. Once within the exchange length of a sufficiently anisotropic magnetic material, a soft magnetic material will find it energetically favorable to align its magnetization with the hard phase. The composite of the two will then function as a permanent magnet with a synergetically enhanced remanence and, ideally, almost the coercivity of the original hard magnetic phase [3]. For the M-ferrites,  $l_{\text{ex}}$  evaluates to about 6 nm [2].

Functioning hard-soft nanocomposite magnets have been realized in numerous experiments, *e.g.* [4, 5], but the particular combination of Fe<sub>3</sub>O<sub>4</sub> and M-ferrites has seen rather limited interest and success [6, 7]. An excellent review on the general subject of nanocomposite magnets can be found in [8].

<sup>a</sup> Corresponding author: jussi.tikkanen@utu.fi

## 2 Experimental

### 2.1 Particle synthesis

SrO·6Fe<sub>2</sub>O<sub>3</sub> nanoparticles were synthesized using a sol-gel combustion method largely based on the work of T. M. H. Dang *et al.* [9]. Unless otherwise stated, reagents of *pro analysi* grade were used at all times.

A 1:11:36 mole fraction mixture of the following ingredients was dissolved into water: strontium chloride hexahydrate, SrCl<sub>2</sub>·6H<sub>2</sub>O, iron(III) nitrate nonahydrate, Fe(NO<sub>3</sub>)<sub>3</sub>·9H<sub>2</sub>O, and citric acid monohydrate, C<sub>6</sub>H<sub>8</sub>O<sub>7</sub>·H<sub>2</sub>O. The solution was homogenized by stirring for one hour, after which a stoichiometric amount of aqueous ammonia solution was added to roughly neutralize the citric acid.

The neutralized solution was stirred for a few more minutes and oven-dried at 90 °C for several days, until a solid orange residue was obtained. The residue was transferred into a well ventilated furnace held at 500 °C, where it ignited and was allowed to remain for 5 h. The resulting gray fluff was annealed at 1050 °C for 2 h in air (heating ramp 1 h), yielding a dark gray powder of nanocrystalline SrO·6Fe<sub>2</sub>O<sub>3</sub>. The furnace was allowed a 5-hour passive cooldown to room temperature before extracting the products.

Microcrystalline SrO·6Fe<sub>2</sub>O<sub>3</sub> particles were produced by an adaptation of the solid-state diffusion method. Strontium nitrate, Sr(NO<sub>3</sub>)<sub>2</sub>, and microcrystalline hematite powder, α-Fe<sub>2</sub>O<sub>3</sub>, were mixed with a few drops of water to dissolve the nitrate. The guideline Sr<sup>2+</sup>:Fe<sup>3+</sup> molar ratio 1:11, optimized for nanoparticles [9], was again followed. The α-Fe<sub>2</sub>O<sub>3</sub> used was not of commercial *pro analysi* grade, but an industrial byproduct provided by *Rautaruukki Oyj*, Finland (XRD purity 100 % ± 1 %, grain size 440 nm).

The wet mixture was annealed at 1200 °C for 2 h (heating ramp 1 h) and given a 5-hour passive cooldown to room temperature. A dark gray batch of slightly fused SrO·6Fe<sub>2</sub>O<sub>3</sub> aggregates was obtained.

A quality control of the SrO·6Fe<sub>2</sub>O<sub>3</sub> and α-Fe<sub>2</sub>O<sub>3</sub> powders was performed by measuring their XRD diffractograms (*Philips X'Pert Pro* diffractometer, Cu K<sub>α</sub> radiation) and magnetic hysteresis loops (*Quantum Design PPMS, ACMS* option) at 300 K. A Rietveld refinement was performed using the *Maud* software [10]. Some essential figures of merit have been collected in table 1 for the SrO·6Fe<sub>2</sub>O<sub>3</sub> powders. A demagnetizing factor  $N = 0.25$  was used when calculating the remanences, determined by measuring the slope of a soft ferromagnetic (Fe<sub>3</sub>O<sub>4</sub>) hysteresis curve near zero external field. The magnetometer samples were rolled into ellipsoids of PTFE tape.

The microparticle synthesis scheme was not optimized to any great extent, and 11 % of the particle mass was left as α-Fe<sub>2</sub>O<sub>3</sub>. This was considered manageable, since the magnetic properties of α-Fe<sub>2</sub>O<sub>3</sub> at 300 K are well known [2] and were easily factored out during analysis based on XRD-determined mass fractions.

**Table 1.** Characteristic figures of SrO·6Fe<sub>2</sub>O<sub>3</sub> precursor powders: nominal diameters ( $d$ ), coercivities of magnetization ( $H_c$ ), remanent magnetizations ( $M_r$ ) and purities by mass.

$d$ (nm)	$H_c$ (kA m <sup>-1</sup> )	$M_r$ (kA m <sup>-1</sup> )	Purity
35	370	185	100 %
440	250	140	89 %

### 2.2 Sample preparation and measurements

Two analogous series of prototype magnets, one with SrO·6Fe<sub>2</sub>O<sub>3</sub> nanoparticles and one with microcrystalline particles, were manufactured by hydraulically dry-compacting the precursor powders (20 min at 30 MPa) and sintering the pellets in a tube furnace (2 h under Ar gas flow at 1050 °C, 1 h heating ramp, 5 h passive cooldown). In addition to the SrO·6Fe<sub>2</sub>O<sub>3</sub> particles, a varying amount of foodstuff-grade potato starch, C<sub>27</sub>H<sub>48</sub>O<sub>20</sub>, was mixed into each sample prior to compaction. The starch was to function as a reductant and partially transform the SrO·6Fe<sub>2</sub>O<sub>3</sub> M-ferrite phase into magnetically softer Fe<sub>3</sub>O<sub>4</sub>.

In summary, both the nanoparticle sample series and the microparticle series contained four pellets, with the amount of starch varying between 0 %, 4 %, 6 % and 9 % by mass. The mass fractions were only fixed to within ± 1 %. The chemical composition and magnetic properties of the pellets were verified by measuring their XRD powder diffractograms and magnetic hysteresis loops at 300 K. Additionally, surface texture measurements were done with the diffractometer in an Eulerian cradle configuration. All samples were found to be crystallographically isotropic.

## 3 Results

The primary basis for evaluating a permanent magnet material lies in its intrinsic working temperature hysteresis loop,  $M(H)$ . As the signal given by the *PPMS ACMS* magnetometer was in terms of effective magnetic moments,  $\mu$ , vs. the external field,  $H_{\text{ext}}$ , the samples were weighed on an analytical balance to the precision of 0.05 mg for converting the data into magnetizations,  $M$ , vs. internal fields,  $H$ . Sample masses were of order of 10 mg.

Considering their powdery nature, the density of the samples was approximated as that of bulk SrO·6Fe<sub>2</sub>O<sub>3</sub>,  $\rho = 5290 \text{ kg m}^{-3}$ , multiplied by the packing factor of a hcp structure,  $\pi/\sqrt{18}$ . Also, the approximate demagnetizing factor  $N = 0.25$  was taken into account. Thus, the total conversion function from measured effective magnetic moments to volume magnetizations took the form

$$M = \frac{\pi\rho\mu}{\sqrt{18}m(1-N)} \quad (2)$$

where  $m$  is the sample mass. Knowing  $M$ , the internal field  $H$  could be calculated from  $H_{\text{ext}}$  and the demagnetizing field,  $H_d \approx -NM$  [2], as

**Table 2.** Figures of merit for the prototype composite magnets: remanent magnetizations,  $M_r$ , coercivities of magnetization,  $H_c$ , and intrinsic maximum energy products,  $BH_{\max}$ . Microparticle series corrected for XRD-determined  $\alpha$ - $\text{Fe}_2\text{O}_3$  content.

Sample	$H_c$ (kA m <sup>-1</sup> )	$M_r$ (kA m <sup>-1</sup> )	$BH_{\max}$ (kJ m <sup>-3</sup> )
nano 0 %	311	191	9.7
nano 4 %	266	200	10.4
nano 6 %	9	123	0.5
nano 9 %	4	35	0.0
micro 0 %	249	154	6.2
nano 4 %	200	198	7.6
nano 6 %	200	183	6.3
nano 9 %	1	99	0.1

$$H = H_{\text{ext}} + H_d \approx H_{\text{ext}} - NM \quad (3)$$

The hysteresis loops measured from both the nanoparticle and microparticle sample series are presented in figure 1. The main figures of merit for each loop can be found in table 2. The  $BH_{\max}$  values given have been calculated as the absolute maxima of the expression

$$-BH = -\mu_0(H + M)H \quad (4)$$

It can be seen that this form of the maximum energy product is, ideally, independent of sample shape, and thus a well-defined material parameter. The leading minus sign was included to give positive  $BH_{\max}$  values, since the extrema in question are reached within the second and fourth quadrants of the hysteresis curves.

Both sample series exhibit a very similar response to the addition of the starch reductant. Remarkably, a modest starch addition was observed to coincide with an increase of the maximum energy product,  $BH_{\max}$ , in both cases vs. the 0 % control sample.

With nanoparticles of  $\text{SrO} \cdot 6\text{Fe}_2\text{O}_3$ , adding 4 % starch increased  $BH_{\max}$  7.2 % from 9.7 kJ m<sup>-3</sup> to 10.4 kJ m<sup>-3</sup>. The energy products were reached at reverse  $H$ -fields of 79.6 kA m<sup>-1</sup> and 81.6 kA m<sup>-1</sup>, respectively. Looking at the corresponding hysteresis loops on the left side of figure 1, it can be seen that a tradeoff between coercivity and remanence has taken place, but in a manner that has been favorable for the  $BH_{\max}$  of the starch-reduced sample. Unfortunately, the mass fraction of  $\text{Fe}_3\text{O}_4$  responsible for the remanence boost was too low to be reliably determined via XRD and Rietveld refinement – it could only be estimated to be below 5 %.

When 6 % starch was added, a very narrow loop was measured, with a prominent constriction around the origin. This curve form is typical of heterogeneous mixtures of magnetically soft and hard components that are poorly exchange coupled [3] – in essence, the linear superposition of two very different hysteresis curves is witnessed. A majority of the  $\text{SrO} \cdot 6\text{Fe}_2\text{O}_3$  particles had been reduced into magnetically soft  $\text{Fe}_3\text{O}_4$ , most of which lay out of the reach of the hard-phase exchange field. Yet more pronounced signs of reductant excess were seen with the 9 % sample. This time, a fraction of the  $\text{Fe}_3\text{O}_4$

was apparently reduced even further into nonmagnetic wüstite,  $\text{FeO}$ .

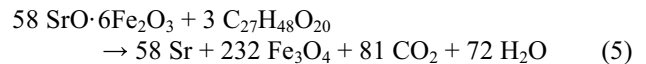
When the  $\text{SrO} \cdot 6\text{Fe}_2\text{O}_3$  nanoparticles were exchanged for microcrystalline particles, a qualitatively similar series of hysteresis loops resulted. Also this time, the addition of 4 % starch improved  $BH_{\max}$  significantly, now by an impressive 22.6 % from 6.2 kJ m<sup>-3</sup> to 7.6 kJ m<sup>-3</sup>.

Based on the huge relative boost and the fact that the 4 % loop's demagnetizing quadrants are just barely convex, one must conclude that the amount of reductant must have been quite optimal. A little bit more starch, and the magnetic phases would have decoupled, as in the 6 % microparticle loop, where slight concave kinks can already be seen in the demagnetizing quadrants. Note, however, that the 6 % sample still exceeded the  $BH_{\max}$  of the 0 % control. With 9 % starch added, the microparticle series ended in a textbook soft magnetic  $\text{Fe}_3\text{O}_4$  hysteresis curve with a minuscule coercivity and a saturation magnetization of order 400 kA m<sup>-1</sup>.

The absolute  $BH_{\max}$  values of the microparticle samples were somewhat smaller than for the analogous nanoparticle composites, owing to the weaker coercivity of the microparticles. The  $BH_{\max}$  values of the 0 % and 4 % samples were reached at  $H$ -fields 61.9 kA m<sup>-1</sup> and 59.5 kA m<sup>-1</sup>, respectively.

## 4 Discussion

To roughly summarize the reduction of  $\text{SrO} \cdot 6\text{Fe}_2\text{O}_3$  into  $\text{Fe}_3\text{O}_4$  by potato starch, the following reaction equation can be proposed:



Apparently, some (liquid) strontium can be expected to be left as an impurity. One should note that  $\text{CO}$ , a gaseous intermediate product and also a reductant, will greatly contribute to the dynamics of the reaction due to its easy diffusion. The reaction is also assumed to take place at the surfaces of solid  $\text{SrO} \cdot 6\text{Fe}_2\text{O}_3$  crystals, making its kinetics very sensitive to particle morphology. Therefore, all in all, the reaction equation (5) can only be taken as a qualitative description of the composite synthesis process.

The fact that the composite is formed by transforming some  $\text{SrO} \cdot 6\text{Fe}_2\text{O}_3$  into  $\text{Fe}_3\text{O}_4$  *in situ* during sintering means that the hard-soft magnetic phase interface will be very clean, allowing efficient interphase exchange coupling. While it is extremely difficult to determine the optimal reductant amount theoretically, it is easy to construct an approximate  $BH_{\max}$  prediction for these composite magnets, based on the Stoner-Wohlfarth model [2].

Let's consider a single spherical core-shell particle magnet, with an interior of  $\text{SrO} \cdot 6\text{Fe}_2\text{O}_3$  and the topmost 10 nm reduced into  $\text{Fe}_3\text{O}_4$ . Although the soft phase layer thickness exceeds the exchange length  $l_{\text{ex}} = 6$  nm given in section 1, it is arguable that this amount of  $\text{Fe}_3\text{O}_4$  could be efficiently exchange-coupled when a multitude of

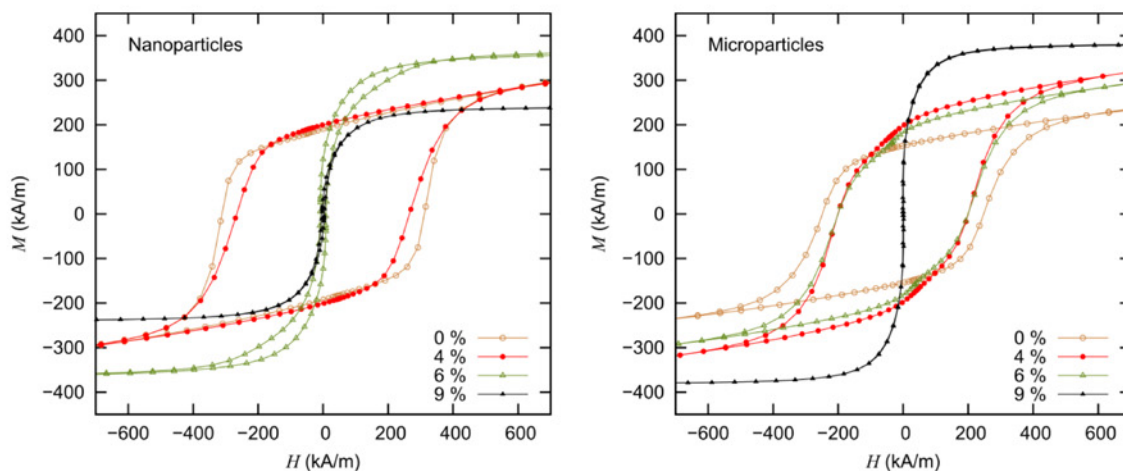


**Figure 1.** The  $M(H)$  hysteresis curves of the nanoparticle series (left) and microparticle series (right), measured at 300 K, with initial starch mass fractions indicated in %. The microparticle curves have been corrected for XRD-determined  $\alpha\text{-Fe}_2\text{O}_3$  content.

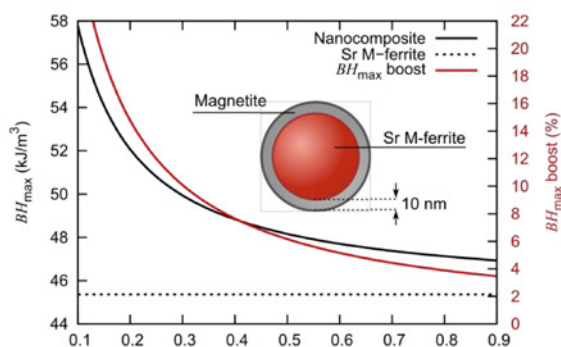


**Figure 2.** An ideal  $BH_{\max}$  prediction for grain-oriented  $\text{SrO}\cdot 6\text{Fe}_2\text{O}_3/\text{Fe}_3\text{O}_4$  core-shell composite magnets (sketch inset) vs. pure  $\text{SrO}\cdot 6\text{Fe}_2\text{O}_3$  M-ferrite.

particles fuse together. Assuming sufficient coercivity and perfect crystal texture, the expression for  $BH_{\max}$  can be simplified to

$$BH_{\max} = \frac{1}{4} \mu_0 M_r^2 \quad (6)$$

The easy-axis remanence of the composite magnet,  $M_r$ , equal to its saturation magnetization in this "square-loop" model, can be approximated as the volume-weighted average of the component bulk magnetizations,  $M_r(\text{SrO}\cdot 6\text{Fe}_2\text{O}_3) = 380 \text{ kA m}^{-1}$  and  $M_r(\text{Fe}_3\text{O}_4) = 480 \text{ kA m}^{-1}$  (data from [2]). Thus, one can plot  $BH_{\max}$  from eq. (6) as a function of particle diameter, as in figure 2. The single-phase M-ferrite prediction ( $BH_{\max} = 45 \text{ kJ m}^{-3}$ ) agrees with published calculations [2]. Further numerical calculations for isotropic Stoner-Wohlfarth magnets suggested a practically identical relative boost curve.

## 5 Conclusions

Through a novel starch reduction method, isotropic hard-soft nanocomposite magnets were synthesized with strontium hexaferrite and magnetite as the hard and soft magnetic phases, respectively. The composites were found to yield maximum energy products that systematically exceeded those of pure  $\text{SrO}\cdot 6\text{Fe}_2\text{O}_3$ , regardless of the size of the  $\text{SrO}\cdot 6\text{Fe}_2\text{O}_3$  particles used as precursors. Using microparticle precursors, the process

could presumably be adapted to yield oriented bulk nanocomposite magnets, whose  $BH_{\max}$  values would theoretically exceed those of pure  $\text{SrO}\cdot 6\text{Fe}_2\text{O}_3$  by over 5%. Promisingly, an experimental  $BH_{\max}$  boost of 23% was observed with isotropic samples.

## 6 Acknowledgements

We acknowledge the Jenny and Antti Wihuri Foundation and Priztech Oy, Finland, for financial support, and especially Martti Paju for valuable industry-specific insights.

## References

1. K. H. J. Buschow (ed.), *Concise Encyclopedia of Magnetic and Superconducting Materials*, 2<sup>nd</sup> ed., 175–183 (Elsevier, Amsterdam, 2005)
2. J. M. D. Coey, *Magnetism and Magnetic Materials*, 234–249, 418–427, 472 (Cambridge University Press, New York, 2009)
3. E. Kneller and R. Hawig, *IEEE Transactions on Magnetics* **27**, 3588–3600 (1991)
4. H. Zeng *et al.*, *Nature* **420**, 395–398 (2008)
5. C. Rong *et al.*, *Applied Physics Letters* **96**, 102513 (2010)
6. P. Bercoff and H. Bertorello, *Journal of Magnetism and Magnetic Materials* **187**, 169–176 (1998)
7. M. Molaei *et al.*, *Journal of Superconductivity and Novel Magnetism* **25**, 519–524 (2012)
8. J. P. Liu *et al.*, *Nanoscale Magnetic Materials and Applications*, 2<sup>nd</sup> ed., 309–332 (Springer, Dordrecht, 2009)
9. T. M. H. Dang *et al.*, *Advances in Natural Sciences: Nanoscience and Nanotechnology* **3**, 025015 (2012)
10. Luca Lutterotti, *Material Analysis Using Diffraction* version 2.33 [computer program] (1997–2011)